MENU 2007
11th International Conference
on Meson-Nucleon Physics and
the Structure of the Nucleon
September10-14, 2007
IKP, Forschungzentrum Jülich, Germany

THREE NUCLEON SCATTERING EXPERIMENTS FROM RIKEN

Kimiko Sekiguchi
RIKEN Nishina Center, Saitama, 351-0198, Japan

Abstract

Recent progress on three nucleon force study with three nucleon scattering at at intermediate energies ($E/A \approx 100$ MeV) are presented, especially focusing on the experimental work on deuteron–proton elastic scattering and breakup reactions at RIKEN. The first signature of three nucleon forces was identified in the cross section minimum for deuteron–proton elastic scattering by direct comparison between the precise data and state of the art Faddeev calculations based on the nucleon–nucleon forces plus the 2π–exchange three nucleon forces. However the polarization observables are not always properly described by adding the three nucleon forces, indicating that components other than 2π–exchange three nucleon forces are required to describe the data.

1 Introduction

A main interest of nuclear physics is to understand the forces acting between nuclear constituents. One recent topic of nuclear force study is to explore the properties of three nucleon forces (3NFs) that appear in the system with more than two nucleons ($A \geq 3$). The 3NFs arise naturally in the standard meson exchange picture, the main ingredient of which is considered to be 2π–exchange with Δ–isobar excitations [1], as well as in the more recent concept of chiral effective field theory. However the effects of the 3NFs are easily masked by those of nucleon–nucleon (NN) forces. Therefore it is hard to approach and find evidences for them experimentally.

The three nucleon (3N) scattering has been studied for a long time as one of the most promising tool to explore the properties of 3NFs since this system provides a rich set of energy dependent spin observables and differential cross sections. At lower energies ($E/A \lesssim 20$ MeV), very high precision measurements were carried out in proton–deuteron (pd) and neutron–deuteron (nd) scattering, including elastic and breakup reactions. However theoretically predicted 3NF effects are rather small and a generally good description

of Nd elastic scattering data is obtained by exact solutions of 3N Faddeev equations employing NN forces only [2, 3] [1]. The situation of the 3NF study have changed since the end of 1990's. The following advances have made us possible to extract the 3NF effects in the 3N scattering.
(i) Establishments of the so-called modern NN forces, e.g. AV18 [4], CD-Bonn [5], Nijmegen I, II and 93 [6], which reproduce a rich set of experimental NN data up to a laboratory energy of 350 MeV with accuracy of $\chi^2 \sim 1$.
(ii) Achievements of rigorous numerical Faddeev calculations based on the modern NN potentials below the π-threshold energy (the incident nucleon energy $E/A \leq 215$ MeV) [2].
(iii) Developments of experimental techniques to obtain precise data of 3N scattering at intermediate energies ($E/A \approx 100$ MeV).
In 1998 indication of 3NF effects in the 3N scattering was first pointed out in the cross section minima for Nd elastic scattering at intermediate energies by the two theory groups [7, 8]. Since then experimental studies of the intermediate–energy pd and nd elastic scattering have been performed intensively by the several facilities, RIKEN, RCNP, KVI, IUCF and Uppsala, providing precise data of cross sections and variety of spin observables [9–14]. The situation would be more interesting in complete dp breakup ($d+p \rightarrow p+p+n$) reactions since they cover different kinematic conditions. By selecting one kinematic configuration, one hopes to enhance the effects which are sensitive to specific amplitudes of the 3NFs. Then the study of dp breakup reactions has followed as the second step of investigation of the 3NF dynamics.

The significance of 3NFs have also been pointed out in nuclear environments other than 3N scattering, e.g. descriptions of the binding of light mass nuclei and the empirical saturation point of the symmetric nuclear matter density. Microscopic calculations, such as the Green's function Monte Carlo [15, 16] and the *ab initio* no-core shell model [17] have been applied to light mass nuclei $A \lesssim 12$ with realistic two– and three– nucleon forces, highlighting the necessity of including 3NFs to explain the binding energies of these nuclei. As for the density of the symmetric nuclear matter it has been reported that all NN potentials provide larger saturation points, and 3NF is taken as one candidate to shift the theoretical results to the empirical point [18].

The current status is in the very beginning of the test ground of the 3NF model. In the following sections, the experimental challenges on dp scattering at RIKEN [9] are presented.

[1] Exceptions are the vector analyzing powers A_y and iT_{11} and the deuteron breakup in the space star configuration.

2 Experiment

2.1 *dp* Elastic Scattering

The experiments for *dp* elastic scattering have been performed at the RIKEN Accelerator Research Facility (RARF). The observables we have covered are cross sections and all deuteron analyzing powers (A_y^d, A_{yy}, A_{xx}, A_{xz}) in the angular range of $\theta_{\mathrm{c.m.}} = 10^\circ - 180^\circ$ at $70 - 135$ MeV/A (deuteron energies of $E_d = 140 - 270$ MeV). Later we have extended the measurement to the deuteron to proton polarization transfer coefficients ($K_y^{y'}$, $K_{xx}^{y'}$–$K_{yy}^{y'}$, and $K_{xz}^{y'}$) and the proton induced polarization $P^{y'}$ at the angles $\theta_{\mathrm{c.m.}} = 90^\circ - 180^\circ$ at 135 MeV/A. Note, the $P^{y'}$ is equivalent with the proton analyzing power A_y^p for the time-reversed reaction $^2\mathrm{H}(\vec{p}, p)^2\mathrm{H}$.

The vector and tensor polarized deuteron beams [19] were accelerated by the AVF and Ring cyclotrons and they bombarded a liquid hydrogen or polyethylene ($\mathrm{CH_2}$) target. Either scattered deuteron or recoil proton was momentum analyzed by the magnetic spectrograph SMART (Swinger and Magnetic Analyzer with Rotator and Twister) [20] depending on the scattering angle and detected at the focal plane (see Fig. 1). For the polarization transfer measurement, the polarization of the elastically scattered protons from the hydrogen target was measured with the focal-plane polarimeter DPOL [21]. The beam polarizations were monitored with the beam line polarimeter by using the analyzing powers for *dp* elastic scattering. To obtain the absolute values of the deuteron beam polarizations, the analyzing powers for *dp* elastic scattering were calibrated by using the $^{12}\mathrm{C}(d,\alpha)^{10}\mathrm{B}^*\,[2^+]$ reaction, the $A_{yy}\,(0^\circ)$ of which is exactly $-1/2$ because of parity conservation [22]. In all the measurements the actual magnitudes of the polarizations were 60–80% of the theoretical maximum values.

Determination of Absolute Values of Cross Section It is essential to get precise absolute values of the cross section to compare with the state of the art Faddeev calculations. However, it is usually difficult to know experimentally the systematic uncertainty. We performed the cross section measurements with the three different experimental setups and tried to estimate the systematic uncertainties. The procedure is as follows. First, we made a measurement at RIKEN with the proton beam at 135 MeV and a $\mathrm{CD_2}$–$\mathrm{CH_2}$ sandwiched solid target at the angles where the *pp* and *pd* elastic scattering were simultaneously measured with the magnetic spectrograph SMART. Using the well-known elastic *pp* cross sections we can estimate the overall systematic uncertainty for the *pd* cross section. Secondly, to confirm the

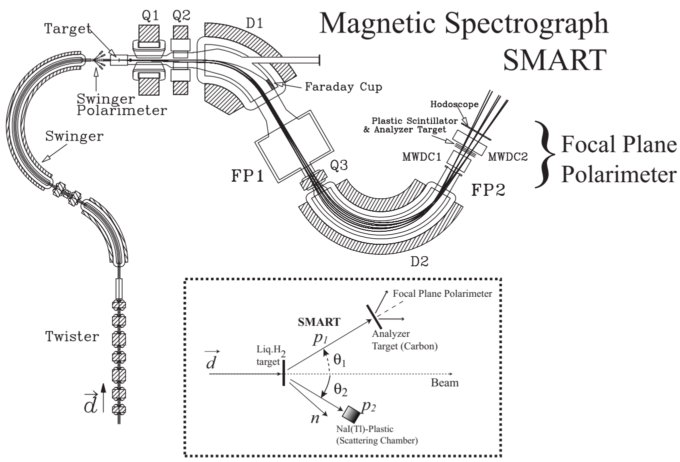

Figure 1: Schematic view of the experimental setup for the measurements on *dp* elastic and breakup processes at RIKEN.

angular distribution we measured with 135 MeV/A deuterons, a CH_2 solid target, and the SMART system. In the measurement we tried to check the fluctuations of the target thickness during the experiment by measuring the *dp* scattering at the fixed angle $\theta_{\text{c.m.}} = 69.7°$, where the scattered deuterons and recoil protons were detected in coincidence in the scattering chamber. For the same purpose, the cross section at $\theta_{\text{c.m.}} = 165.1°$ was measured with the SMART system over several times during the experiment. Lastly, we performed a totally independent measurement at the Research Center for Nuclear Physics (RCNP) of Osaka University, using a 135 MeV proton beam and deuterated polyethylene target. The absolute normalization of the cross sections has been performed by taking data with a D_2 gas target and the double slit system for which the RCNP group has already established the procedure to obtain the absolute *pd* cross section [10]. All the experimental results are shown in Fig. 2. The data taken at RCNP are shown with black solid diamonds. The open squares are the data measured with the proton beam at RIKEN and the open circles are the data with the deuteron beam at the same laboratory. Only statistical errors are presented. The very good agreement between the independent measurements allows us to conclude that the systematic uncertainty due to the detection setup is small [9].

2.2 *dp* Breakup Reaction

The breakup experiment was also performed with the SMART spectrograph using polarized deuteron beams at 135 MeV/A. The measurement was focused on the deuteron to proton polarization transfer coefficient $K_{yy}^{y'}$ and all deuteron analyzing powers for the specific coplanar configurations to study the model dependence of 3NFs. The angle sets of the two scattered protons (p_1, p_2) were ($\theta_1 = 27°$–$33°$, $\theta_2 = 31°$, $\phi_1 - \phi_2 = 180°$). The two emerging protons were detected in coincidence to identify the *dp* breakup events. The p_1 was momentum analyzed by the magnetic spectrograph SMART and its polarizations were measured with the focal plane polarimeter. The p_2 was detected by the E–dE counters consisting of NaI(Tl) and plastic scintillators installed in a scattering chamber (see Fig. 1). The kinetic energies were covered from 164 MeV–180 MeV for the p_1 and 30 MeV–75 MeV for the p_2, respectively.

3 Results and Discussion

Cross Section in elastic *dp* scattering First, we compare the cross section data for elastic *dp* scattering with the theoretical predictions. The data at 135 MeV/A are shown with open circles in the Fig. 2 together with the Faddeev calculations by the Bochum-Cracow-KIT (BCK) group. The red (blue) shaded band in the figure shows the calculations with (w/o) Tuscon-Melbourne 99 (TM99) [23] based on the modern NN potentials, namely CD-Bonn, AV18, Nijmegen I, II. The solid line is the calculation based on the AV18 potential plus the Urbana IX 3NF [24]. Note the main ingredients of these two 3NFs are two-pion exchange with Δ–isobar excitations. Based on the comparison between the data and the NN force predictions, the clear discrepancies are found in the angular range where the cross sections take minimum at the measured incident energies 70 and 135 MeV/A (the data at 70 MeV/A are not shown here). They become larger as the incident energy increases. The discrepancies are explained by taking into account the 2π exchange type 3NF models (TM99, and Urbana IX). All 2π-exchange 3NF potentials considered here provide 3NF effects for the cross section which are comparable in magnitude and sign.

Another alternative theoretical predictions have been reported by the Hannover-Lisbon group in which the Δ–isobar excitations are explicitly included in the coupled-channel approach [25]. The contributions are based on all meson exchanges, i.e. π, ρ, σ, and ω exchanges contained in the coupled-channel approach. Thus the π–π, π–ρ, ρ–ρ with with Δ–isobar excitations as well as the Illinois type [16] many-π rings are incorporated effectively. The CDBonn potential was taken as the NN interaction. Recently this group has succeeded in incorporating the Coulomb forces via the screening and renormalization approach in the momentum-space framework [26]. The results are shown in Fig. 2. The dashed curve in cyan is the coupled-channel approach prediction obtained with the Δ–isobar excitations and the dotted curve in cyan is the prediction in which the Coulomb interactions are additionally included. The predictions with the NN forces only are not shown in the figures since they provide the similar results to those on the CDBonn potential by the BCK group. The Δ-isobar effects improve the agreement in the angular range where the cross sections take minimum as is similar to the results by the BCK group. It should be noted that the very nice agreements are found at the very forward angles by taking into account the Coulomb forces.

The theoretical approach to estimate the effects other than 3NFs is also in progress. The BCK group have recently reported the calculations with the Lorentz boosted NN potentials [27, 28] to estimate the relativistic effects in 3N scattering. For the cross section in elastic Nd scattering their effects are restricted at the very backward angles, indicating that the 3NF is the only plausible mechanism to resolve the discrepancies between NN theory and the experimental data in the cross section minimum.

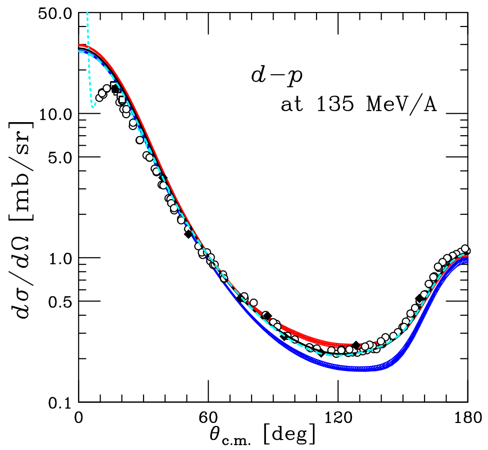

Figure 2: Cross section for dp elastic scattering at 135 MeV/A. For the descriptions of the theoretical predictions, see text.

Polarization Observables in Elastic dp Scattering Parts of the polarization observables in dp elastic scattering are shown with open circles in Fig. 3. The statistical errors are only shown in the figure and their values are less than 0.03 for all the measured observables. Generally, the discrepancies between the data and the pure NN force predictions (blue shaded bands) are clearly seen at the angles where the cross sections take minimum. However the predictions based on NN + 3NF not always provide better descriptions of the data. The agreements are improved by incorporating the TM99 or Urbana IX 3NF for the proton analyzing power A_y^p and the polarization transfer coefficient $K_{xx}^{y'} - K_{yy}^{y'}$, while for the tensor analyzing powers A_{xx} and A_{yy}, differences between the data and the NN force predictions are not reproduced by adding the 3NFs. The Δ-isobar effects (dashed curves in cyan) are similar to those of the TM99 and Urbana IX 3NFs for almost all observables except for the tensor analyzing power A_{xx} for which the prediction with the Δ–isobar provides a better agreement.

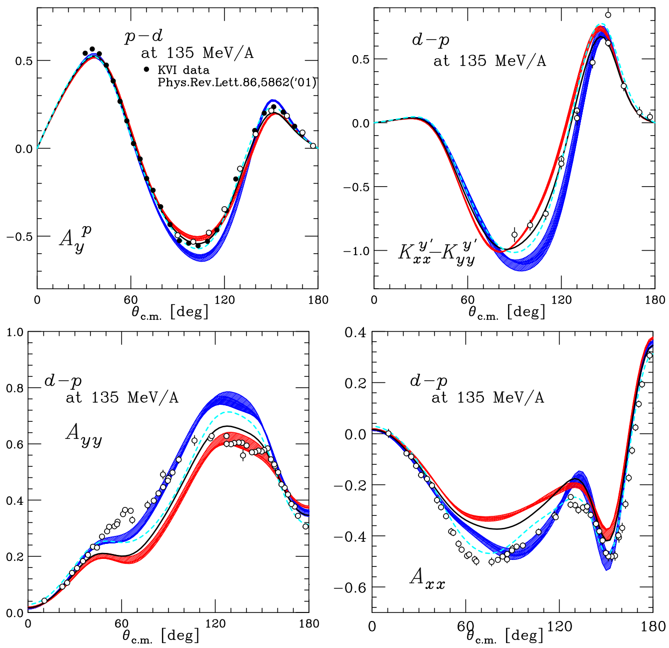

Figure 3: Proton and deuteron analyzing powers and polarization transfer coefficients for dp elastic scattering at 135 MeV/A. For the descriptions of the theoretical predictions, see text.

Polarization Observables in dp Breakup Reactions In Fig. 4 the experimental results are shown with open circles along with the kinematic curves of the emerging two protons (S-curve). The statistical errors are only shown and they are less than 0.03 for all the measured observables. The data were obtained with the S–curve energy bin of 8 MeV for the analyzing powers and 12 MeV for the polarization transfer coefficients. The predictions shown here are averaged over the S-curve energy bin of 8 and/or 12 MeV for the direct comparison between the data and the calculations. For the polarization transfer $K_{yy}^{y'}$, the inclusions of the 3NFs change the shapes of the predictions from those on the pure NN forces (a blue shaded band) drastically. The different results are predicted between the TM99 3NF (a

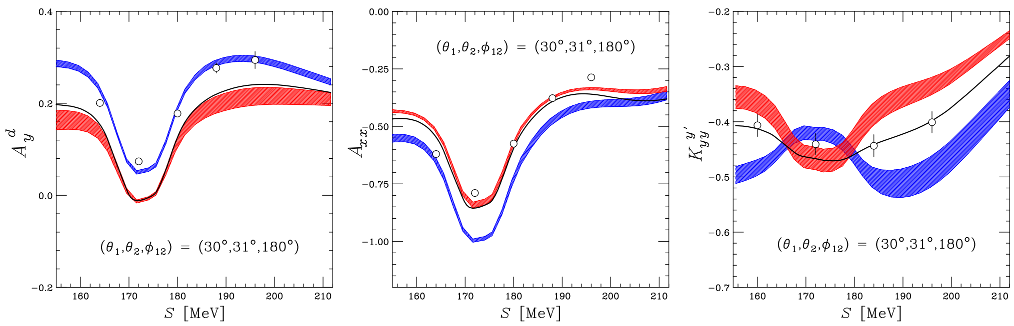

Figure 4: Analyzing powers (A_y^d, A_{xx}) and deuteron to proton polarization transfer coefficient $K_{yy}^{y'}$ for the dp breakup reaction at 135 MeV/A. For the descriptions of the theoretical predictions, see text.

red shaded band) and the Urbana IX 3NF (a solid curve). The data rather support the predictions with the Urbana IX 3NF. For the tensor analyzing power A_{xx} the agreements are improved by adding the TM99 or Urbana IX 3NFs, however for the vector analyzing power A_y^d the agreement is deteriorated by taking into account the 3NFs. The data are well reproduced by the predictions with the NN forces only. It is interesting to note that the results are opposite to what has been seen in elastic dp scattering.

The cross section data for elastic dp scattering have opened up a new possibility to explore 3NFs via the 3N scattering at intermediate energies. The results of spin observables both for dp elastic and breakup reactions indicate insufficient understanding of spin dependent parts of 3NFs. It would be interesting to see how well the theoretical approaches, e.g. addition of 3NFs other than 2π exchange types, relativistic treatment, and the potentials based on chiral effective field theory [29] describe these obtained data.

4 Summary

The 3NFs are now taken as key elements to understand various nuclear phenomena, such as the binding of light mass nuclei and the empirical saturation point of nuclear matter density. The Nd scattering provide rich sources to explore the properties of 3NF such as momentum and spin dependences. Since the end of 1990's extensive experimental measurements on proton–deuteron and neutron–deuteron elastic scattering at intermediate energies ($E/A \approx 100$ MeV) have been performed at several facilities. Study of Nd breakup reactions has followed as the second step. In this talk, the experimental work on *dp* elastic scattering and *dp* breakup reactions at RIKEN was presented. Comparing the data with state of the art Faddeev calculations one concludes that the cross section data for elastic *dp* scattering are explained by incorporating 2π–exchange 3NFs, what is the first clear signature of 3NF effects in the three nucleon scattering. However polarization observables are not always properly described by adding the 3NFs, indicating that additional components are required to describe the data. To understand these spin observables, theoretical approaches incorporating 3NFs other than 2π exchange types, relativistic treatment, incorporating of coulomb effects, and completely new approach based on chiral effective field theory are now in progress.

Acknowledgments

This work has been performed in collaboration with RIKEN, the University of Tokyo, RCNP, Tokyo Institute of Technology, KVI, Kyushu University, Saitama University, Jagiellonian University, Ruhr-Universität Bochum, Kyushu Institute of Technology, Forschungszentrum of Jülich, Universität Hannover, and Universidade de Lisboa.

References

[1] J. Fujita, and H. Miyazawa, Prog. Theor. Phys. **17**, 360 (1957).

[2] W. Glöckle, H. Witała, D. Hüber, H. Kamada and J. Golak, Phys. Rep. **274**, 107 (1996).

[3] A. Kievsky, M. Viviani, and S. Rosati, Phys. Rev. C **64**, 024002 (2001).

[4] R. B. Wiringa *et al.*, Phys. Rev. C **51**, 38 (1995).

[5] R. Machleidt, Phys. Rev. C **63**, 024001 (2001).

[6] V. G. J. Stoks *et al.*, Phys. Rev. C **49**, 2950 (1994).

[7] H. Witała *et al.*, Phys. Rev. Lett. **81**, 1183 (1998).

[8] S. Nemoto *et al.*, Phys. Rev. C **58**, 2599 (1998).

[9] N. Sakamoto *et al.*, Phys. Lett. B **367**, 60 (1996); H. Sakai *et al.*, Phys. Rev. Lett. **84**, 5288 (2000); K. Sekiguchi *et al.*, Phys. Rev. C **65**, 034003 (2002); K. Sekiguchi *et al.*, Phys. Rev. C **70**, 014001 (2004); K. Sekiguchi *et al.*, Phys. Rev. Lett **95**, 162301 (2005).

[10] K. Hatanaka *et al.*, Phys. Rev. C **66**, 044002 (2002).

[11] R. Bieber *et al.*, Phys. Rev. Lett. **84**, 606 (2000); K. Ermisch *et al.*, Phys. Rev. Lett. **86**, 5862 (2001); K. Ermisch *et al.*, Phys. Rev. C **68**, 051001 (2003); K. Ermisch *et al.*, Phys. Rev. C **71**, 064004 (2005); H. R. Amir-Ahmadi *et al.*, Phys. Rev. C **75**, 041001 (2007); H. Mardanpour *et al.*, Eur. Phys. J. A **31**, 383 (2007).

[12] E. J. Stephenson *et al.*, Phys. Rev. C **60**, 061001 (1999); R. V. Cadman *et al.*, Phys. Rev. Lett. **86**, 967 (2001); B. v. Przewoski *et al.*, Phys. Rev. C **74**, 064003 (2006).

[13] P. Mermod *et al.*, Phys. Rev. C **72**, 061002 (2005).

[14] Y. Maeda *et al.*, Phys. Rev. C **76**, 014004 (2007).

[15] R. B. Wiringa *et al.*,Phys. Rev. C **62**, 014001 (2000).

[16] S. C. Pieper *et al.*, Phys. Rev. C. **64**, 014001 (2001).

[17] P. Navrátil and W. E. Ormand, Phys. Rev. C **68**, 034305 (2003).

[18] see for example, A. Akmal *et al,*, Phys. Rec. C **58**, 1804 (1998).

[19] H. Okamura *et al.*, AIP Conf. Proc. **293**, 84 (1994).

[20] T. Ichihara *et al.*, Nucl. Phys. **A569**, 287c (1994).

[21] S. Ishida *et al.*, AIP Conf. Proc. **343**, 182 (1995).

[22] K. Suda *et al.*, Nucl. Instrum. Methods Phys. Res. A **572**, 745 (2007).

[23] S. A. Coon and H. K. Han, Few Body Syst., **30**, 131 (2001).

[24] B. S. Pudliner *et al.*, Phys. Rev. C**56**, 1720 (1997).

[25] A. Deltuva *et al.*, Phys. Rev. C **68**, 024005 (2003).

[26] A. Deltuva *et al.*, Phys. Rev. C **71**, 054005 (2005).

[27] H. Kamada *et al.*, Phys. Rev. C **66**, 044010 (2002).

[28] H. Witała *et al.*, Phys. Rev. C 71, 054001 (2005).

[29] E. Epelbaum Prog. Part. Nucl. Phys. **57**, 654 (2006).